

Network Sharing: a pathway to Sustainability and Carbon Footprint Mitigation in Radio Access Networks

Daniela Renga¹, Michela Meo¹, Loutfi Nuaymi²

¹ Politecnico di Torino, Torino, Italy

² IMT Atlantique, Rennes, France

Abstract—The extensive densification of radio access networks (RANs) aims to cope with the staggering increase in mobile traffic demand. However, this process raises remarkable concerns due to the resulting growth in RAN energy consumption and the associated carbon footprint. This paper examines the potential of network sharing (NS) among mobile network operators (MNOs) as a sustainable alternative to network densification, addressing energy and environmental challenges in RAN operation. By enabling the recurrent deactivation of base stations (BSs) during periods of low traffic demand, NS offers a promising approach to reduce energy consumption. We investigate the energy savings achievable under two NS strategies across various area types, analyzing the impact of dynamically adjusting NS parameters over time. Additionally, the interplay between BS sleep mode duration and the frequency of BS switching operations reveals conflicting effects on BS degradation. Our study evaluates these effects, demonstrating how the proposed NS strategies can effectively extend BS lifetimes. In addition to energy savings, our results highlight the significant benefits of NS in mitigating the RAN carbon footprint, achieved through reductions in both operational and embodied carbon emissions.

Index Terms—Network sharing, Sustainability, Carbon footprint

I. INTRODUCTION

The transition towards the 5G and beyond era is marked by the widespread penetration of extremely demanding communication services that are characterized by the exchange of huge traffic volumes, high bandwidth requirements, and tight delay constraints. As a result, the staggering growth of traffic demand observed in radio access networks (RANs) is expected to persist unabated in the coming years. In fact, global mobile data traffic is projected to exceed 300 Exabyte per month by 2029, nearly tripling compared to 2023 [1]. The typical approach adopted by mobile network operators (MNOs) to cope with a similar scenario is represented by the densification of RANs. However, this process raises significant sustainability concerns in relation to the substantial increase in energy demand, especially considering that, despite the energy-efficient design of 5G network devices, the overall

energy consumption of 5G RANs is anticipated to significantly surpass that of 4G RANs [2]. This, in turn, results in a significant financial impact for MNOs, given that the RAN is responsible for over 50% of the energy consumption both in 4G and 5G networks, and that the RAN power supply currently accounts for up to 80% of MNO operational expenditures (OPEX) [3]. In addition, the capital expenditures (CAPEX) required to install additional network nodes in RANs are far from negligible for MNOs. Moreover, relevant concerns arise in relation to the impact of RAN densification in terms of carbon footprint. Communication networks are responsible for up to 35% of all ICT carbon emissions, which alone constitute almost 4% of the global carbon emission [4]. Physical and regulatory constraints may prevent the boundless expansion of RANs, especially in urban environments.

In this context, Network Sharing (NS) emerges as a promising solution to foster more sustainable deployment and operation of RANs. Under the NS paradigm, multiple MNOs collaborate to share their network infrastructures, enabling cooperative management of network resources. This allows customers of any participating MNO to seamlessly access the network infrastructure owned by other MNOs involved in the agreement. The purposes for implementing NS are manifold. First, they include energy saving, due to the deactivation of unused network nodes during periods of low traffic, which is enabled by the consolidation of the traffic demand on few network nodes shared by different MNOs [5], [6]. Second, besides reducing OPEX through the decrease of energy demand during the RAN operation, NS agreements among different MNOs enable a more effective network planning. In particular, by limiting the need for installing new network nodes to cope with traffic peaks, NS allows to reduce CAPEX for MNOs [5], [7]. In addition, NS is emerging in the literature as a solution to enable the deployment of resilient RANs, particularly as new vulnerabilities arise in RANs due to the rapid expansion of communication infrastructures and the heightened risk of electric grid overload, which increases the likelihood of power supply unavailability [8].

Our study focuses on the potential of NS to enable a sustainable deployment and operation of 5G and beyond RANs. We propose a NS strategy to dynamically offload traffic between base stations (BSs) that belong to different MNOs and happen to be co-located, i.e., they are installed on the same site. This NS approach allows to consolidate traffic on

This work was partially supported by the European Union under the Italian National Recovery and Resilience Plan (NRRP) of NextGenerationEU, partnership on “Telecommunications of the Future” (PE00000001 - program “RESTART”, focused project R4R).

few BSs and deactivate those nodes that do not carry any traffic. With respect to our previous work [6], we expand our investigation of the NS performance considering wider portions of RANs, several types of traffic areas and multiple combinations of MNOs, to provide a more in-depth analysis of the impact of different traffic profiles and the capacity shared by the BSs. Furthermore, this paper investigates the potential of NS not only in terms of achieved energy saving, that was not specifically addressed in [8], but also focusing on the effects of switching on/off operations on the BS degradation. Indeed, BS activation and deactivation procedures entail variations of the BS operation temperature, possibly leading to more likely failures of BS hardware components. Conversely, the periods in which the BS is put in sleep mode tend to preserve the BS lifetime to a variable extent. However, the sensitiveness of a BS hardware to the frequency of switching operations and to the duration of sleep mode periods may vary depending on the BS technology, hence leading to possibly different impacts of NS in terms of BS lifespan duration and cost due to the need for BS replacement [9]. We extensively analyze how varying the NS parameter settings affect the NS performance, depending on the traffic profiles and the amount of capacity shared among BSs. Moreover, we evaluate whether dynamically varying NS configuration settings based on the period of the day may contribute to enhance the balance among energy saving, switching frequency and BS degradation. Finally, we investigate the benefits of NS on reducing the RAN carbon footprint, taking into account not only carbon emissions due to the energy demand for RAN operation, but also the embodied carbon emissions due to the manufacturing, transportation and end-of-life management of BSs.

II. THE NETWORK SHARING APPROACH

In this section we describe the case study scenario investigated in our work, also detailing the traffic offloading strategies designed to implement NS in a RAN. As sketched in Fig. 1, we consider a portion of a RAN in an urban environment in which two MNOs provide mobile access service to their customers within the same coverage area. To reduce the energy demand of the RAN, we propose a traffic offloading strategy enabled by the sharing of the network infrastructure among different MNOs, based on a predefined agreement. The NS strategy is applied on pairs of co-located BSs (i.e., installed on the same site) owned by two different MNOs. In this work, two BSs from different operators are assumed to be co-located if they are placed sufficiently close to each other to provide a nearly overlapping coverage ($\geq 95\%$) over the same area. In each pair, the NS strategy envisions that the BS characterized by having the largest bandwidth capacity is assumed to be continuously kept active. Let us assume that this BS is owned by the operator indicated as Op_1 . Conversely, at each time step the other BS, owned by Op_2 , can be deactivated if both the following conditions hold:

- 1) the traffic handled by Op_2 BS can be transferred to the nearby BS owned by Op_1 without saturating its nominal capacity above a predefined threshold, denoted by C_{th} ;
- 2) the first condition holds for at least the next w time steps,

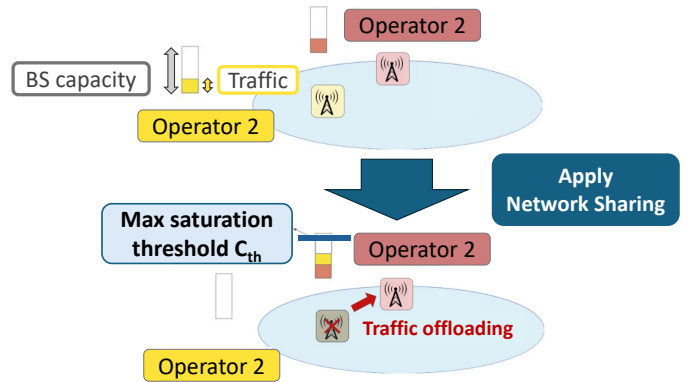


Fig. 1: Network sharing: if the traffic is sufficiently low, traffic is offloaded to a co-located BS of another operator, provided that its capacity is not saturated over the threshold C_{th} .

meaning that during this time period the aggregated traffic volume from Op_1 and Op_2 BSs results sufficiently low to be effectively consolidated on a single BS, i.e., Op_1 BS, without violating the BS capacity constraint. This condition guarantees that once the Op_2 BS is put into sleep mode, its reactivation is not required before a minimum time window has elapsed, so as limit the frequency of BS on/off switching operations.

This study is conducted under the assumption of perfect knowledge of the future traffic demand, as traffic predictions can actually be quite accurate as shown in [10]. We define a *Standard version* of the proposed NS strategy, denoted *SNS*, based on which C_{th} and w are kept constant during NS operation. Then, we introduce a *Dynamic version* of the described NS strategy, that we name *DNS*. The latter method represents a simple yet effective approach to more effectively adapt to the fluctuating characteristics of traffic demand across various times of the day. According to the DNS strategy, two distinct configurations are defined for C_{th} and w : one applies during daytime (8 am-8:00 pm), while the other one is set for nighttime (8 pm-8:00 am).

III. SYSTEM MODEL

For the analysis we consider the city of Lyon, France and we focus on sample pairs of BSs owned by two different MNOs. As concerns traffic volumes, we consider the NetMob dataset [11]. The dataset contains real traces of normalized mobile traffic provided by a French mobile operator. The traffic patterns cover a period of 77 days, with samples collected every 15 minutes with a spatial resolution of 100×100 m², and report more than 60 different mobile services. Real data about the geographical distribution of sites hosting mobile BSs, with information about the adopted mobile technology and the owner MNOs (Bouygues, Free Mobile, Orange, SFR) for each BS are retrieved from public datasets made available by the Agence Nationale des Fréquences (ANFR) [12]. Fig. 2 depicts the distribution of traffic volume over the entire city, with warm shades closer to red indicating higher normalized traffic volumes and cold nuances corresponding to low traffic areas. The actual location of the BSs owned by the MNO that provided the traffic traces is represented by black dots; we denote this operator as Op_1 . As expected, BSs appear

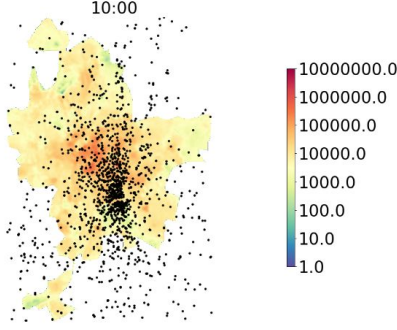


Fig. 2: Sites of Op_1 BSs and traffic volume intensity in the city of Lyon at 10 am.

more densely deployed in the city center, whereas a lower BS density characterizes the peripheral and suburb areas.

As in our previous work [6], we consider traces of downlink traffic generated by the most demanding services (i.e., Video Streaming, Social Media, App Store, Web Browsing, Cloud, Music, and Gaming), corresponding to 29 different types of applications.

To derive realistic traces of the traffic volumes handled by the BSs of Op_1 that are located in the considered areas, we map the traces of traffic volumes distributed over the tiles to each of the BSs of Op_1 included in the considered area, based on a Voronoi tessellation approach. The traffic trace representing the actual traffic volumes handled by each BS B_i is derived from the aggregation of the traffic data series associated as described above. The aggregated traffic trace is further scaled up by a factor f_C that is proportional to the actual BS bandwidth capacity, making the conservative assumption that the peak of the aggregated normalized traffic volume should correspond to 90% of the overall estimated BS capacity.

In addition to BSs from Op_1 , based on the ANFR data [12], we consider the BSs from a different MNO, namely Op_2 . As already mentioned, we consider only co-located BSs, i.e., BSs sharing the same site, which are about 30% of the total. Each of these BSs is assigned an aggregated traffic volume trace based on the same processing method presented above. In order to avoid correlation of the derived traffic traces among different MNOs, all the elements in the traffic time series derived for each Op_i are shifted by $i \cdot N$ positions with respect to the original trace, with N corresponding to the number of time slots in a week.

IV. ENERGY AND OTHER SUSTAINABILITY CONSIDERATIONS

We now describe the modeling approach for BS energy consumption within the considered scenario. Additionally, we outline the impact of NS on BS degradation, detailing the model used to assess how time spent in sleep mode and the frequency of switching operations affect BS lifetime. Finally, we present a model to evaluate the influence of NS on the RAN carbon footprint, encompassing contributions from both embodied and operational carbon emissions.

A. Energy consumption model

The energy consumption of the BS is evaluated using the well-established power models outlined in [13], specifically for LTE technology, and considering a Radio Remote Head (RRH) BS. The power consumption required by the BS during its operation, denoted as P_{in} , is estimated as follows:

$$P_{in} = N_{TX} \cdot (P_0 + \Delta_p \cdot P_{out}), \quad 0 \leq P_{out} \leq P_{max} \quad (1)$$

where N_{TX} is the number of transceivers, P_{max} represents the maximum radio frequency output power at full load, P_0 corresponds to the fixed power consumption when the radio frequency output power is null, and Δ_p is the slope of the load dependent power consumption; P_{out} is the radio frequency output power due to the actual BS load, denoted as ρ , and it is expressed as:

$$P_{out} = \rho \cdot P_{max}, \quad 0 \leq \rho \leq 1 \quad (2)$$

The value of the BS load ρ actually corresponds to the BS traffic load normalized with respect to the maximum traffic amount that can be handled by the BS given its capacity. The consumption of the BS in sleep mode is assumed negligible. In our study, we assume the typical parameter settings adopted to characterize the consumption of LTE RRH macro BSs, as detailed in [13]: $N_{TR}=6$; $P_0=130$ W; $P_{max}=20$ W; $\Delta_p=4.7$. The energy demand of a BS b_i over an observation period of K time slots, that we denote E^i , is hence derived as:

$$E^i = \sum_{k=1}^K P_{in_k}^i \cdot \Delta T \cdot x_k^i \quad (3)$$

where $P_{in_k}^i$ is the average power consumption of BS b_i during time slot k , ΔT is the time slot duration, and x_k represents a binary variable indicating whether the considered BS is active ($x_k^i=1$) or in sleep mode ($x_k^i=0$) in the current time slot k .

To assess the contribution of NS to reduce the energy consumption of RANs, we define a key performance indicator (KPI), denoted by S_E , to estimate the energy saving that can be obtained for a pair of co-located BS when NS is applied. For each pair of BSs (i.e., b_i and b_j), this metric is computed as follows:

$$S_E = 1 - \frac{E_{NS}^i + E_{NS}^j}{E_{BL}^i + E_{BL}^j} \quad (4)$$

where E_{BL}^i and E_{BL}^j represent the energy demand of BSs b_i and b_j , respectively, in the baseline scenario (the BSs are always kept active), whereas E_{NS}^i and E_{NS}^j represent the energy demand of the two BSs when NS is applied.

B. Impact of NS on BS degradation

In addition to supporting sustainability goals in RAN operation by saving energy during periods in which a BS is deactivated, NS may also impact the BS lifespan and failure rate. On the one hand, putting a BS in sleep mode entails a decrease of its operating temperature, hence contributing to reduce the failure rate and preserving the BS lifetime [14]–[16]. On the other hand, any BS transition from an active state to a sleep mode, and vice versa, entails a power state change that negatively impacts the BS failure rate. Indeed, depending on

the metal sensitivity to temperature variations and to state cycling, the failure rate of a BS may increase by frequent switching operations [17].

A metric adopted in the literature to quantify the impact of switching operations and periods in sleep modes on the BS lifetime is represented by the Accelerator Factor (AF) [9], [14], [18]. This indicator provides the mean lifetime increase/decrease with respect to the always on condition, with values of AF larger than 1 corresponding to increased failure rate and decreased BS lifespan, vice versa for values lower than 1. For each BS b_i , the AF can be computed over a period of duration θ , as follows:

$$AF_{i,\theta} = 1 - \underbrace{(1 - AF_{sleep})\tau_{sleep}}_{\text{Lifetime Increase}} + \underbrace{\chi f}_{\text{Lifetime Decrease}} \quad (5)$$

where AF_{sleep} is the AF, computed assuming that the device is always kept in sleep mode - according to [16], AF_{sleep} is always lower than 1, otherwise putting the device in sleep mode would mean increasing the failure rate of the device. Then, τ_{sleep} is the fraction of time slots the BS has spent in sleep mode in the period of duration $\theta = K \cdot \Delta T$. The parameter f , in cycle/h, is the frequency of the switching cycle which is measured over θ . Finally, χ , in h/cycle, acts as weight of the frequency f and is defined as $(\gamma_b^{on} N_F)^{-1}$, where γ_b^{on} , in failure/h, is the failure rate when the BS is active, computed with the Arrhenius law [16], whereas N_F , in cycle/failure, is the number of cycles supported by the device before a failure occurs. In Equation 5, two opposing contributions are highlighted: one associated with the time spent in sleep mode, τ_{sleep} , which reduces the AF and thereby extends the BS lifetime, and another one linked to the switching frequency, which exerts a contrary effect on the AF and subsequently shortens the BS lifetime [9]. The parameters χ and AF_{sleep} depend on the hardware component used to build the BS, while τ_{sleep} and f depend on the switching strategy. Finally, the expected lifetime of BS b_i under NS operation, denoted as L_i , can be expressed as follows:

$$L_i = AF_{i,\theta} \cdot L_i^{active} \quad (6)$$

where L_i^{active} represents the expected lifetime of BS b_i assuming the BS remains continuously active.

C. Carbon footprint

In this study, we also want to assess the impact of NS on the carbon footprint of the RAN compared to standard RAN operation. Specifically, we analyze the carbon emission intensity associated with a BS both in the baseline scenario and under NS. To provide a comprehensive evaluation of the carbon footprint, we take into account two components: operational carbon emissions from BS activity and embodied emissions from BS manufacturing, transportation, and end-of-life treatment. Operational carbon emissions depend on the carbon intensity, which is defined as the amount of carbon emissions produced per unit of consumed energy. The carbon intensity, in turn, may vary significantly across different countries, based on the energy mix used to power the network. We assume a carbon intensity of 265 gCO₂e/kWh for the

EU, based on data from the European Environment Agency (EEA) in 2022 [19], and 390 gCO₂/kWh for the US, according to the US Energy Information Administration (EIA) [20]. To assess the embodied carbon emissions we refer to [21], from which we derive an annual carbon emission intensity of 782 kgCO₂e/year for a single BS, based on the provided data. This estimate takes into account both the radio unit and the baseband unit, assuming a BS lifespan of 8 years [21]. Clearly, the application of NS on a BS pair contributes to decrease their carbon footprint, due to the reduction of energy demand. Furthermore, NS may affect the annual embodied carbon emission intensity. Indeed, depending on the frequency of switching operations and on the fraction of time spent in sleep mode under NS, the value of AF for a BS that is periodically switched on and off under NS is variably affected, leading to an increase or decrease of the BS lifetime. As a result, the annual embodied carbon footprint, that is computed assuming an expected BS lifespan of 8 years, is decreased (or increased) if the value of the AF leads to an increased (or decreased) BS lifespan.

To quantify the impact of NS on the carbon footprint, we define the following KPIs:

1) *Operational Carbon emission intensity* - I_O : this metric represents the average carbon emission intensity per year due to the energy consumption of a pair of co-located BSs owned by different MNOs to which NS can be applied. Considering a pair of BSs b_i and b_j , it is computed as follows:

$$I_O = I_C \cdot K_{year} \cdot (\bar{E}_{\Delta T}^i + \bar{E}_{\Delta T}^j) \quad (7)$$

where I_C is the carbon intensity per unit of energy, K_{year} is the number of time slots in a year. \bar{E}^i and \bar{E}^j correspond to the mean energy demand per time slot of BS b_i and of BS b_j , respectively, and they are derived as $\bar{E}_{\Delta T}^i = E^i K^{-1}$ and $\bar{E}_{\Delta T}^j = E^j K^{-1}$, with K representing the number of time slots in the observation period.

2) *Embodied Carbon emission intensity* - I_E : this metric represents the average carbon emission intensity per year due to BS manufacturing, transportation and end-of-life treatment, for a pair of co-located BSs owned by different MNOs to which NS can be applied. Considering a pair of BSs b_i and b_j , it is derived as follows:

$$I_E = I_E^i + I_E^j \quad (8)$$

where I_E^i and I_E^j represent the yearly carbon emission intensity for each BS in the considered pair. To provide the definition of I_E^i , let us first denote by $I_{E,tot}^i$ the total embodied carbon emission intensity for a single BS b_i , which is the sum of all carbon emissions associated with the BS's manufacturing, transportation, and end-of-life management. Then, we denote with $I_{E,year}^i$ the total embodied carbon emission intensity for a single BS, $I_{E,tot}^i$, normalized by the BS lifetime. It is hence computed as:

$$I_{E,year}^i = \frac{I_{E,tot}^i}{L^i} \quad (9)$$

where L^i indicates the expected BS lifetime of BS b_i , expressed in years. Finally, for a BS b_i , I_E^i can be defined as:

$$I_E^i = I_{E,year}^i \cdot AF^i \quad (10)$$

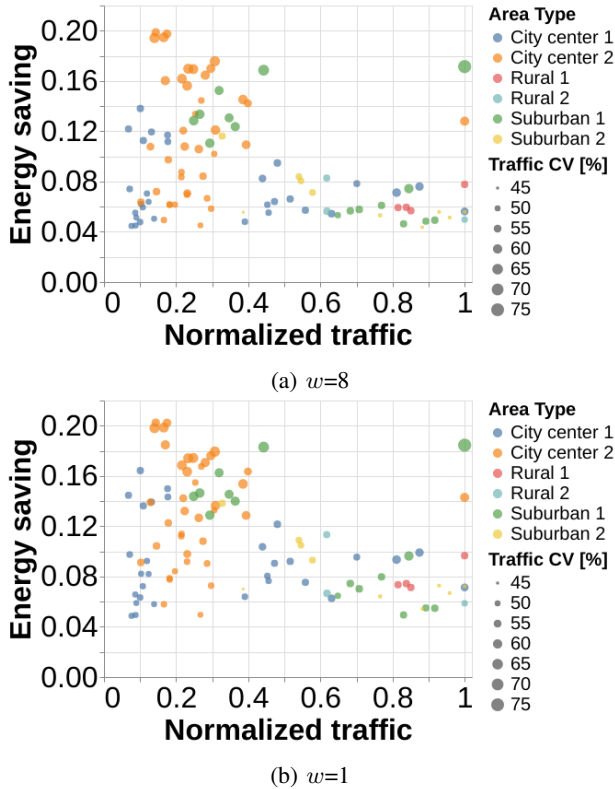


Fig. 3: Energy saving under different settings of sleep window w considering several BS pairs in different traffic areas.

where AF^i is the accelerator factor of BS b_i in the considered scenario (i.e., baseline or under NS application). In this equation, scaling the value of $I_{E,year}^i$ with AF^i allows to take into account the potential impact of NS to increase or decrease the expected BS lifespan. Notice that AF is 1 for any BS when no NS is applied.

V. IMPACT OF ENERGY SAVING

We first present the performance analysis carried out to investigate the contribution of the proposed SNS strategy to reduce the RAN energy consumption. We consider two different city center areas (*City center 1*, *City center 2*), two suburban areas (*Suburban 1*, *Suburban 2*), and two rural areas (*Rural 1*, *Rural 2*). The size of each identified area is 20×20 tiles (4 km^2), in order to include in our investigation a reasonable number of BSs, that are operated by four different Mobile Operators (Bouygues, Free Mobile, Orange, SFR). The BS density results 26.25 BSs per km^2 in the urban areas, 7.88 BSs per km^2 in the suburban areas, and 3.63 BSs per km^2 in the rural areas. Within each area, we consider all the possible pairs of colocated BS from all possible combinations of MNO pairs (for a total of 6 different MNO pairs). Our simulations are conducted over a period of one month, considering time slots of 15 minutes.

A. Impact of SNS parameter configuration

Fig. 3 shows the energy saving obtained under SNS in different area types (represented by different colors), assuming a saturation threshold $C_{th}=0.7$. Two different values of minimum sleep window w are considered, i.e., $w=8$ (Fig. 3a) and

$w=1$ (Fig. 3b), corresponding to 2 hours and 15 minutes, respectively. The energy savings are reported versus the average traffic volume per time slot handled by each considered BS pair b_i and b_j , that we denote $v_{i,j}$. This traffic volume is normalized with respect to the maximum value observed across the entire set of analyzed BS pairs. The size of the points in the graph is proportional to the coefficient of variation (CV) of the traffic volume carried by each BS pair. Results in Fig. 3a show that energy savings may vary quite a lot depending on the area types, with up to 20% energy saved in the City center 1. More than 4% of energy can be saved under SNS in any area type. The average traffic volume per BS pair does not seem to significantly influence the energy savings that can be achieved in BS pairs whose traffic features low CV, whereas a higher traffic variability, entailed by larger values of CV, allows to achieve the largest savings. When w is set to a lower value (Fig. 3b), the energy savings result only slightly reduced, suggesting a limited impact of this parameter on the energy saving achievable under NS. This may be due, first, to the fact that the largest contribution to the energy saving is obtained during the night, when the traffic is typically very low and one of the two BS, once deactivated, can be kept in sleep mode for long periods of time. Second, during the daytime, in a context in which BS capacity typically results underutilized, it is unlikely that, after a BS deactivation in a pair, the traffic volume raises again above the threshold C_{th} before two hours.

We now investigate the impact of varying the setting of the threshold C_{th} on energy saving. Similarly to Fig. 3, Fig. 4 depicts the energy savings obtained under SNS for BS pairs in different area types versus the normalized average traffic per BS pair, assuming different configurations of the saturation threshold, i.e., $C_{th}=0.5$ (Fig.4a), $C_{th}=0.7$ (Fig.4b), and $C_{th}=0.9$ (Fig.4c). The value of w is set to 1 (corresponding to 15 minutes). We find that, as the capacity threshold increases, the energy savings tend to become larger. The more evident benefits derived from increasing C_{th} emerge for those BS pairs that, under conservative settings of the capacity threshold (i.e., $C_{th}=0.5$), features the lowest values of sleep time, τ_{sleep} (data not reported for sake of brevity). For example, some BS pairs in the City center 2 exhibit a value of τ_{sleep} of about 0.25 under $C_{th}=0.5$, whereas under $C_{th}=0.9$ the sleep time nearly doubles, mirroring the increase observed in energy savings. Conversely, BS pairs that achieve substantial energy savings even under conservative capacity threshold settings gain little additional benefit from further increasing the threshold. This is exemplified by certain BS pairs from City Center 1, where energy savings increase by approximately 10%. In these cases, the sleep time exceeds 0.9 even when $C_{th}=0.5$.

B. Analysis under dynamic NS strategy

We now analyse the performance under dynamic NS strategy, DNS. Fig. 5 illustrates a heat map matrix that represents the energy savings obtained under DNS for three sample BS pairs from different area types, with different hues corresponding to varying levels of energy saving. Each row represents a different combination for the settings of C_{th} and w that can

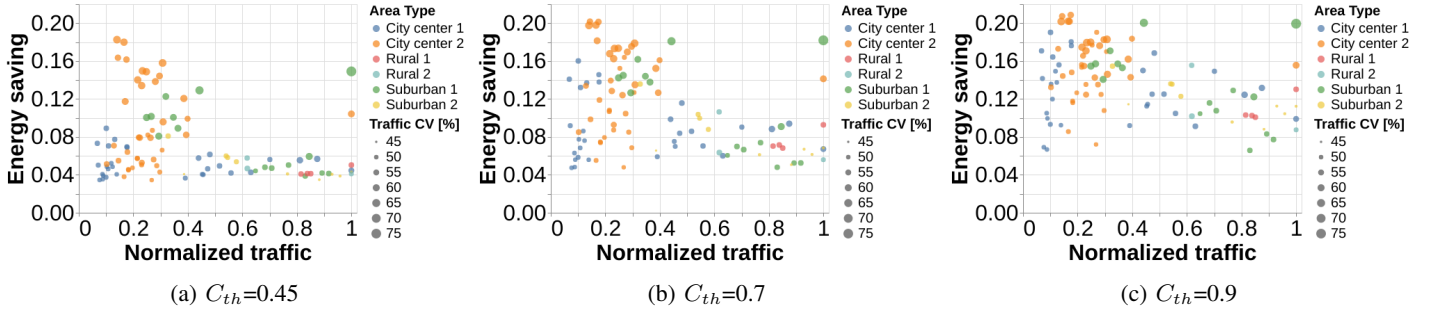


Fig. 4: Energy saving under different settings of capacity threshold C_{th} considering several BS pairs in different traffic areas.

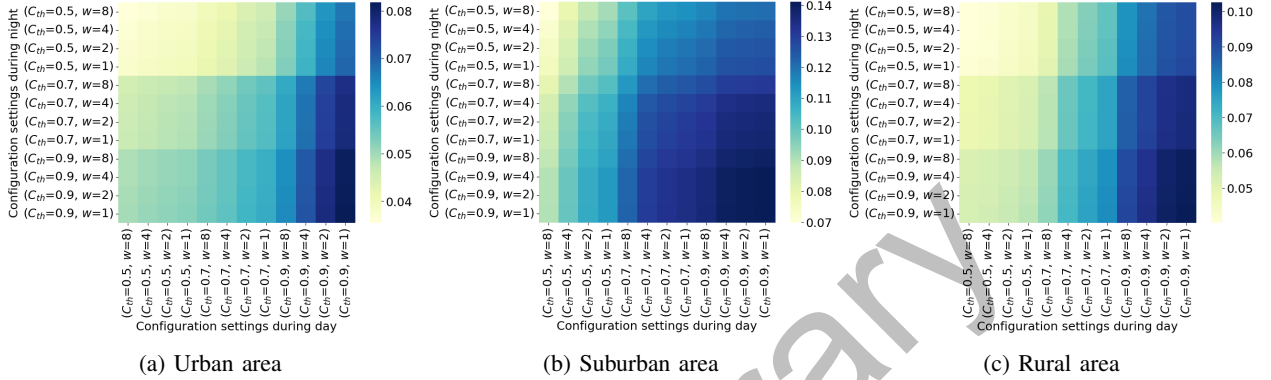


Fig. 5: Energy saving under dynamic NS settings, for sample BS pairs in a urban, suburban and rural area.

be adopted during the night period, with $C_{th}=\{0.5, 0.7, 0.9\}$ and $w=\{1,2,4,8\}$. Similarly, each column corresponds to a different configuration of the NS parameters applied during the day time. Finally, each element in the matrix defines the combination of the DNS parameter settings, including both those adopted during the night and those adopted during the day, that are tested in our study. Varying the setting of the sleep window shows a higher impact during the day, especially under intermediate to high values of C_{th} for urban and rural areas, and under lower setting of C_{th} for the suburban area. Small values of w are more beneficial to reduce the energy demand. Conversely, the impact of varying w during the night is negligible, except for the suburban area. In general, the highest savings are obtained in the suburban area, even under conservative settings of C_{th} . This behavior is likely due to a lower traffic demand combined with a lower correlation between traffic traces of the two BSs in the suburban pair.

Furthermore, these results show that in terms of energy saving the DNS strategy does not provide significant benefits, since the largest energy saving are achieved applying the same configuration settings, i.e., $C_{th}=0.9$ and $w=1$, during the daytime and during the night period. However, as discussed in next section, Sec. VI-VII, focusing on other types of metrics, like the switching frequency and the accelerator factor, a different trend may be observed, possibly requiring to set distinct combinations of parameter settings during the day and during the night to better trade off conflicting goals (e.g., sustainability versus BS lifetime).

VI. NS EFFECTS ON BS LIFETIME

We now evaluate the effects of NS on the BS lifetime. First, Fig. 6 reports the BS switching frequency recorded under DNS

for a BS that, in a pair of co-located BSs, is periodically deactivated. This metric is shown for three different area types, under several combinations of parameter settings during the daytime and during the night. The setting of w shows a more relevant impact with respect to the case of energy saving. Furthermore, it exhibits an opposing behavior, since lower settings of w , that may yield higher energy savings, provide high values of BS switching frequency, which are not advisable due to their negative impact in terms BS degradation. Notice that in suburban areas, the DNS settings that provide the largest energy savings also ensure a limited BS switching frequency. In contrast, in urban and rural areas, these factors are decoupled, with greater energy savings achievable only at the cost of a higher BS switching frequency.

To more accurately assess the impact of NS on BS lifetime, we analyze the acceleration factor, AF, of the BS that, in a pair of co-located BSs, is periodically deactivated under NS. This indicator quantifies the increase in the BS failure rate due to NS, accounting for both the beneficial effects of the time a BS spends in sleep mode and the negative impact associated with the frequency of BS switching operations. To this aim, Fig. 7a depicts the values of AF measured under DNS for a BS in a pair representative of a suburban area. We assume $AF_{sleep} = 0.2$ and $\chi = 0.5$, as measured in [9] for an LTE BS. AF is decreased by NS under any parameter configuration with respect to the case in which NS is not applied. The lowest values of AF, resulting in an extended BS lifetime, are observed under high C_{th} setting. However, it is not convenient to reduce w below 2 neither increasing it up to 8, especially during the day. Values of w that result in a minimum sleep window between 30 and 60 minutes enable a more effective balance between the conflicting dynamics entailed by BS

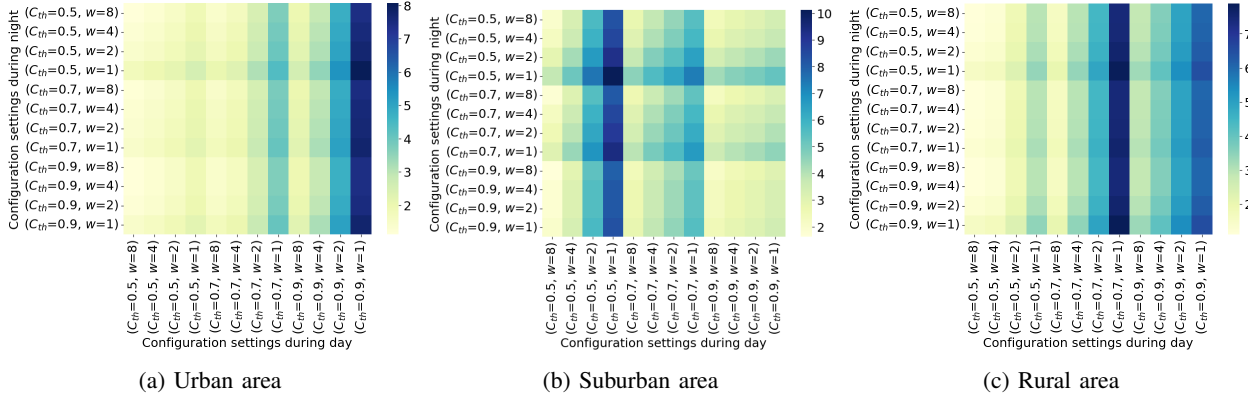


Fig. 6: BS switching frequency under dynamic NS settings, for sample BS pairs in a urban, suburban and rural area.

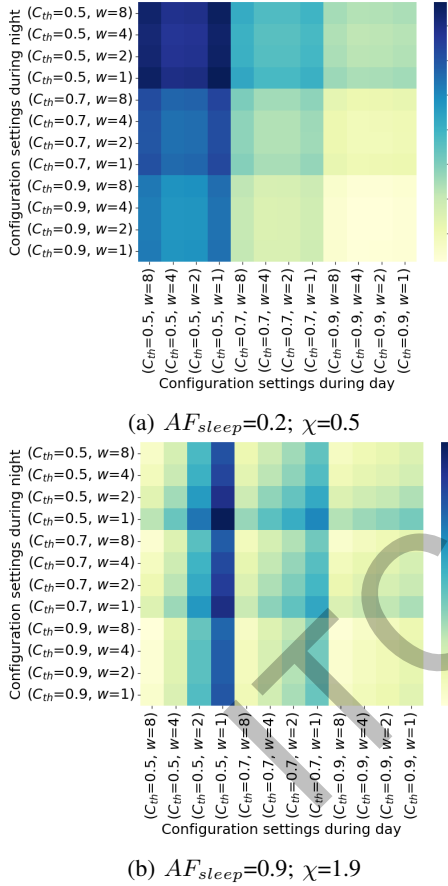


Fig. 7: Acceleration factor assuming different configurations of AF_{sleep} and χ under dynamic NS settings, for the BS that, in a sample BS pair from a suburban area, is periodically deactivated under NS.

switching frequency and sleep time under NS. This ensures the minimization of the AF, given the configuration of C_{th} , thus preserving the BS lifetime. We remark that an AF decrease may also contribute to limit the management cost associated to the BS replacement at the end of its lifetime.

As previously mentioned, the setting of AF_{sleep} and χ depends on the BS technology. Variations in these parameter settings can lead to significantly different AF outcomes for the BS impacted by switching operations under NS. In fact, Fig. 7b shows the AF observed for the same BS assuming

$AF_{sleep} = 0.9$ and $\chi = 1.9$, that are considered representative of a pessimistic scenario, since the sleep mode only slightly decrease the BS failure rate whereas the BS switching operations significantly affect the BS deterioration [18]. In this case, the value of AF increases under all DNS parameter configurations, leading to a reduction of the BS lifetime. Furthermore, higher values of w help minimize the resulting AF, with $w=8$ effectively limiting the AF increase, even at low C_{th} levels—unlike the case analyzed in Fig. 7a.

VII. ESTIMATION OF NS EFFECT ON CARBON EMISSIONS

We now investigate the contribution of NS to mitigate the RAN carbon footprint. Fig. 9 illustrates the operational and embodied yearly carbon emission intensity for all pairs of co-located BSs across all the area types. The figure compares the baseline (BL) scenario, where no NS is applied, with the scenario in which SNS is implemented ($C_{th}=0.9, w=2$), assuming $AF_{sleep}=0.2$ and $\chi=0.5$. The BS pairs, shown along the x-axis, are sorted based on their energy demand in the BL scenario. The operational carbon emission intensity is presented for both the EU and US energy mixes. The operational carbon emission intensity in the BL scenario increases as the energy demand of the BS pair rises, reaching nearly 50% higher values for the US energy mix compared to the EU. NS allows to reduce I_O by up to more than 18%, with larger decrease observed for BS pairs that exhibit a lower energy demand when no NS is applied. The reduction in I_O for the analyzed BS pairs under SNS does not follow a monotonic trend as in the BL scenario. This is because it is directly influenced by the sleep time of the BS that is periodically deactivated, which, in turn, is highly dependent on traffic profiles. These profiles can vary significantly, even for BS pairs with similar energy demands in the BL scenario. Finally, we note that in the BL scenario the yearly embodied carbon emission intensity of the considered BS pairs, which is influenced by the expected BS lifetime, can account for more than half of the operational carbon emission intensity. Hence, by reducing the embodied carbon emission intensity by up to more than one-third (orange curve), NS makes a significant contribution to lowering the share of embodied emissions in the total RAN carbon footprint.

Focusing on a pair of co-located BSs representative of a suburban area, Fig. 8 shows the embodied carbon emissions, I_E , measured under DNS for increasing values of the ob-

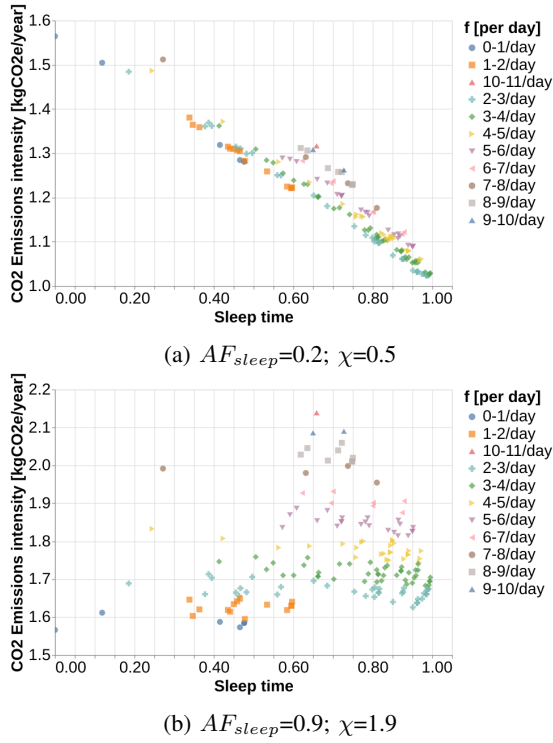


Fig. 8: Embodied CO2 emission intensity under different NS configuration settings, for a BS pair in a suburban area, considering different settings of AF_{sleep} and χ .

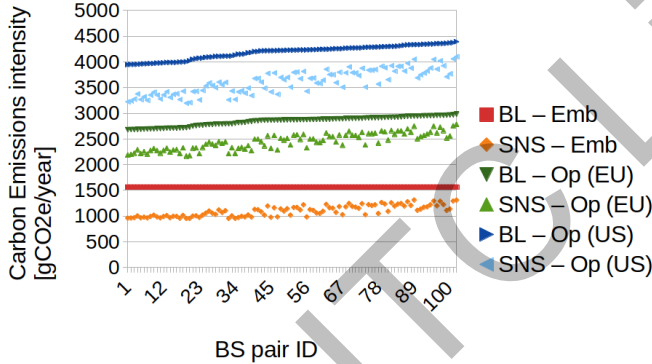


Fig. 9: Embodied (Emb) and Operational (Op) Carbon Emissions intensity assuming $AF_{sleep}=0.2$ and $\chi=0.5$ under dynamic NS configuration settings, for all BS pairs in all area types, sorted for increasing energy saving under NS, considering EU and US energy mixes.

served sleep time (for the BS that is periodically deactivated), comparing different settings of AF_{sleep} and χ . Each point represents a different configuration of the DNS parameters (the same combinations of settings considered for the results reported in Fig. 5-7), whereas the colors (corresponding to different symbols) indicate the various ranges of the switching frequency (f) values, as registered for the BS that is periodically switched off. Under $AF_{sleep}=0.2$ and $\chi=0.5$ (Fig.8a), the value of I_E tends to decrease as the sleep time grows larger. DNS settings which result in higher BS switching frequency tend to yield slightly smaller decrease in I_E , given the same value of the sleep time. Conversely, under pessimistic settings of AF_{sleep} and χ (Fig.8b), the values of I_E result significantly

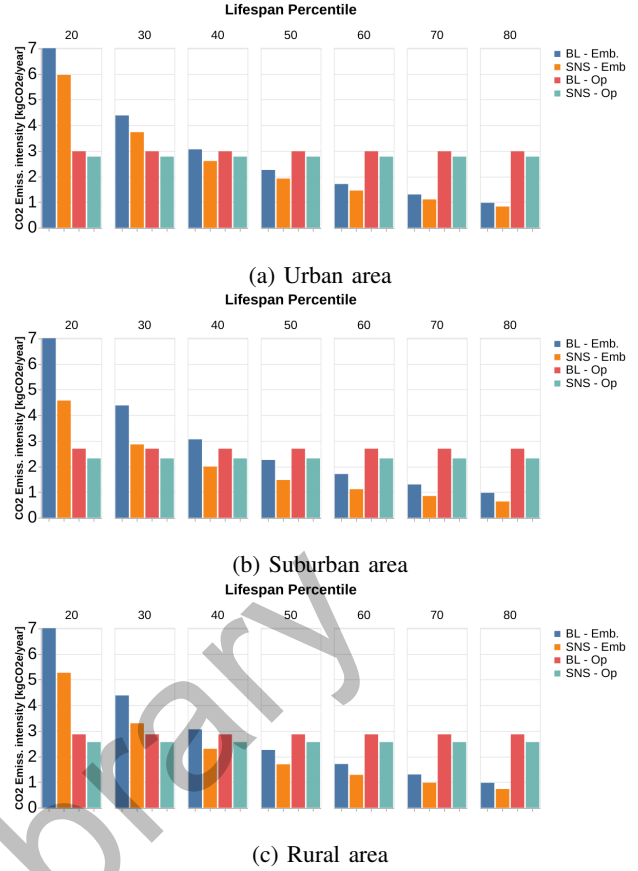


Fig. 10: Embodied (Emb) and Operational (Op) Carbon emissions intensity assuming LTE technology under NS with $C_{th}=0.9$ and $w=1$, for different percentiles of expected BS lifetime, considering sample BS pairs in a urban, suburban and rural area.

higher than the previous case, exhibiting an opposite trend, where peak values are reached with relatively high sleep times. However, for a given range of f , I_E shows minimal sensitivity to variations in sleep time, while increased values of f significantly raise the embodied carbon emission intensity. This behavior aligns with the limited impact of sleep mode on reducing AF under these settings of AF_{sleep} and χ , coupled with the detrimental effect of higher switching frequency on AF. This results in a shorter expected lifetime for the BS undergoing periodic deactivations, which consequently leads to a higher overall embodied carbon emission intensity for the considered BS pair.

Finally, we consider the effects of NS on the carbon footprint, focusing on how they may depend on the expected lifetime of the BSs in the BL scenario. Indeed, the expected lifetime of a set of BSs can be modeled with an exponential distribution, characterized by an average value of 8 years in our case study. Considering three different area types, Fig. 10 reports the embodied and operational carbon emission intensity, both for the BL scenario and under SNS ($C_{th}=0.9$, $w=1$). Fig. 10a represent the different types of carbon emission intensity for a sample BS pair representative of an urban area, in the BL scenario and under SNS. Each subplot displays the results for the considered BS pair, making the following

assumption about the expected lifetime of the two BSs in the BL scenario, i.e., when no NS is implemented. For the BS that is always kept active, the expected lifetime is 8 years. In contrast, the expected lifetime of the BS undergoing periodic deactivations, that we denote L^* , corresponds to a given percentile of an exponential distribution with an average value of 8 years. The specific percentile for each subplot is indicated at the top. Similarly, Fig. 10b-10c show the same analysis for BS pairs in the suburban and rural areas. We observe that for values of L^* below the 40-th percentile, the embodied carbon emission intensity, I_E , accounts for more than half the total carbon footprint (embodied and operational) of the BS pair, resulting up to more than doubled with respect to I_O in the BL scenario. In these cases, the reduction of I_E enabled by NS provides a substantial contribution to mitigate the carbon footprint of the considered BS pair. As the expected lifetime in the BL scenario increases (higher percentiles), the contribution of I_E to the total carbon footprint progressively decreases, up to resulting one third of I_O for the 80-th percentile of L^* . Furthermore, these results highlight that, in terms of fractional reduction, NS is more effective in lowering the carbon footprint associated with embodied carbon emissions than in lowering that associated with BS operation. This demonstrates NS's significant contribution to enabling a more sustainable RAN operation.

VIII. CONCLUSIONS

This paper explores the potential of NS to foster more sustainable RAN operations, with a particular focus on balancing sustainability objectives and the impact of NS on BS lifetime. Specifically, the interaction between the time a BS spends in sleep mode and the frequency of BS switching operations creates conflicting effects on BS degradation. Our results demonstrate that, by properly configuring NS parameters, significant energy savings of over 20% can be achieved without negatively impacting the BS failure rate. Furthermore, our findings show that NS is highly effective in reducing not only the operational carbon footprint of the RAN but also the embodied carbon emissions, which often make up a substantial portion of the total carbon footprint. In fact, NS's ability to extend BS lifetime leads to a significant reduction in embodied carbon emissions. Finally, dynamically adjusting the NS parameter configuration over time enables a more effective balance between sustainability objectives and the adverse impacts of NS operation on BS lifetime and embodied carbon emissions intensity. This approach is particularly advantageous when the BS technology exhibits high sensitivity to switching operations. However, further research is needed to better understand how traffic characterization influences NS performance in meeting sustainability goals. Additionally, varying outcomes in terms of BS degradation are observed depending on BS technology, highlighting the need for NS strategies tailored to specific RAN scenarios, particularly those involving the coexistence of heterogeneous mobile technologies. Finally, our study could be updated in the future with additional carbon footprint models.

REFERENCES

- [1] Ericsson, "Ericsson Mobility Report November 2024," November 2024. [Online]. Available: <https://www.ericsson.com/en/reports-and-papers/mobility-report/reports/november-2024>
- [2] C.-L. I, S. Han, and S. Bian, "Energy-efficient 5G for a greener future," *Nature Electronics*, vol. 3, pp. 182–184, 2020.
- [3] Next G Alliance, "Green G: The Path Toward Sustainable 6G," 2022. [Online]. Available: <https://access.atiss.org/higherlogic/ws/public/download/63277>
- [4] M. Bettiol, M. Capestro, E. Di Maria, and S. Micelli, "At The Roots Of The Fourth Industrial Revolution: How ICT Investments Affect Industry 4.0 Adoption," in "Marco Fanno" Working Papers 0253, Dipartimento di Scienze Economiche "Marco Fanno", 2020.
- [5] N. Slamnik-Kriještorac, H. Kremlo, M. Ruffini, and J. M. Marquez-Barja, "Sharing distributed and heterogeneous resources toward end-to-end 5g networks: A comprehensive survey and a taxonomy," *IEEE Communications Surveys Tutorials*, vol. 22, no. 3, pp. 1592–1628, 2020.
- [6] D. Renga, M. Ni, M. Ajmone Marsan, and M. Meo, "Network Sharing to Enable Sustainable Communications in the Era of 5G and Beyond," in *ICC 2024 - IEEE International Conference on Communications*, 2024, pp. 2840–2846.
- [7] W. W. Priambodo, H. Wijanto, and N. M. Adriansyah, "Techno-economics analysis of ran-spectrum sharing scheme use sensitivity analysis method," in *2023 International Conference on Computer Science, Information Technology and Engineering (ICCoSITE)*, 2023, pp. 679–684.
- [8] D. Renga, M. Ni, M. Ajmone Marsan, and M. Meo, "Sharing rans for energy efficiency," in *2024 IEEE 25th International Workshop on Signal Processing Advances in Wireless Communications (SPAWC)*, 2024, pp. 706–710.
- [9] L. Chiaraviglio, F. Cuomo, M. Listanti, E. Manzia, and M. Santucci, "Fatigue-aware management of cellular networks infrastructure with sleep modes," *IEEE Transactions on Mobile Computing*, vol. 16, no. 11, pp. 3028–3041, 2017.
- [10] G. Vallero, D. Renga, M. Meo, and M. A. Marsan, "Greener RAN Operation Through Machine Learning," *IEEE Transactions on Network and Service Management*, vol. 16, no. 3, pp. 896–908, 2019.
- [11] O. E. Martínez-Durive, S. Mishra, C. Ziemlicki, S. Rubrichi, Z. Smoreda, and M. Fiore, "The NetMob23 dataset: A high-resolution multi-region service-level mobile data traffic cartography," arXiv:2305.06933 [cs.NI], 2023.
- [12] "Agence Nationale des Fréquences (ANFR)," [Online]. Available: <https://data.anfr.fr>, <https://cartoradio.fr> [Accessed on 28 June 2023]
- [13] G. Auer, O. Blume, V. Giannini, I. Godor, M. Imran, Y. Jading, E. Kastranaras, M. Olsson, D. Sabella, P. Skillermark *et al.*, "D2.3: Energy efficiency analysis of the reference systems, areas of improvements and target breakdown," *Earth*, vol. 20, no. 10, 2010.
- [14] L. Chiaraviglio, F. Cuomo, M. Listanti, E. Manzia, and M. Santucci, "Sleep to stay healthy: Managing the lifetime of energy-efficient cellular networks," in *2015 IEEE Global Communications Conference (GLOBECOM)*. IEEE, 2015, pp. 1–7.
- [15] L. Chiaraviglio, P. Wiatr, P. Monti, J. Chen, J. Lorincz, F. Idzikowski, M. Listanti, and L. Wosinska, "Is green networking beneficial in terms of device lifetime?" *IEEE Communications Magazine*, vol. 53, no. 5, pp. 232–240, 2015.
- [16] S. Arrhenius, "About the reaction speed during the inversion of cane sugar by acidic acids," *magazine for physical chemistry*, vol. 4, no. 1, pp. 226–248, 1889.
- [17] Y.-L. Lee, J. Pan, R. Hathaway, and M. Barkey, *Fatigue testing and analysis: theory and practice*. Butterworth-Heinemann, 2005, vol. 13.
- [18] G. Vallero, D. Renga, M. Meo, and M. A. Marsan, "Ran energy efficiency and failure rate through ann traffic predictions processing," *Computer Communications*, vol. 183, pp. 51–63, 2022. [Online]. Available: <https://www.sciencedirect.com/science/article/pii/S0140366421004400>
- [19] European Environment Agency, "Greenhouse gas emission intensity of electricity generation," 2024. [Online]. Available: <https://www.eea.europa.eu/en/analysis/maps-and-charts/co2-emission-intensity-15>
- [20] U.S. Energy Information Administration, "How much carbon dioxide is produced per kilowattour of U.S. electricity generation?" 2023. [Online]. Available: <https://www.eia.gov/tools/faqs/faq.php?id=74t=11>
- [21] J. Malmodin and N. Lövehagen, "A methodology for simplified lcas of electronic products," in *2024 Electronics Goes Green 2024+ (EGG)*, 2024, pp. 1–12.